Z. Kristallogr. **215** (2000) 10–16

# The crystal structure of synthetic buckhornite, $[Pb_2BiS_3][AuTe_2]$

H. Effenberger*, [I], F. J. Culetto[II], D. Topa[III] and W. H. Paar[III]

[I] Universität Wien, Institut für Mineralogie und Kristallographie, Althanstraße 14, A-1090 Vienna, Austria
[II] Kärntner Elektrizitäts AG, Arnulfplatz 2, A-9021 Klagenfurt, Austria
[III] Universität Salzburg, Institut für Mineralogie, Hellbrunnerstraße 34, A-5020 Salzburg, Austria

Received February 24, 1999; accepted May 26, 1999

**Abstract.** Synthetic buckhornite, $[Pb_2BiS_3][AuTe_2]$, was grown from melts in connection with the search for high-temperature superconductive materials. Chemical analyses were performed by electron-microprobe investigations. The crystal structure was determined from 726 single-crystal X-ray reflections of a twinned crystal. The refinement gave $R(F) = 0.101$ for 33 variable parameters. The space group is $Pmmn$, $a = 4.108(3)$ Å, $b = 12.308(9)$ Å, $c = 9.331(6)$ Å, $Z = 2$. The atomic arrangement features a pronounced layer structure formed by two different sheets. (a) Planar $Au^{[4Te]}Te_4$ configurations are edge-connected to ribbons in [100]; they are linked by $Te \cdots Te$ contacts to planar nets parallel to (001). Te and Au atoms are in a distorted square arrangement. (b) Slices of (Pb,Bi)S are sandwiched between these $AuTe_2$ layers. They form SnS-archetype layers.

The present paper proves that buckhornite, $[(Pb_2Bi)_{\Sigma 3}S_3][(Te_2Au)_{\Sigma 3}]$, and nagyagite, $[(Pb_3(Pb,Sb)_3)_{\Sigma 6}S_6][(Te,Au)_3]$ are members of a homologous series. Both compounds have comparable Au–Te layers. However, ordering of Au and Te atoms was verified in buckhornite only. In buckhornite *two* (Pb,Bi)S sheets form one slice of the SnS-archetype whereas in nagyagite *four* (Pb,Sb)S layers form the corresponding slice with a thickness of two SnS-archetype slabs.

## Introduction

The mineral buckhornite was described by Francis, Criddle, Stanley, Lange, S'how Shieh and Francis (1992) after acceptance as a new species by the Commission on New Minerals and Mineral Names (International Mineralogical Association). The holotype material from Boulder County, Colorado, had been collected more than 50 years earlier. The authors described occurrence, morphology, optical behaviour, X-ray powder data, cell metrics and the chemical composition $AuPb_2BiTe_2S_3$. Precession X-ray films showed an orthorhombic cell and systematic extinctions indicating the presence of a glide plane; a tetragonal subcell was evident. Francis *et al.* (1992) refined the cell parameters from an X-ray powder pattern: $a = 4.092(2)$ Å, $b = 12.245(4)$ Å, $c = 9.322(4)$ Å; based on additional weak powder lines violating the extinction rule the authors assumed the extinction symbol $P$- - - for buckhornite. Close relationships between buckhornite and nagyagite were derived from similarities of physical properties, X-ray data and chemical formula which suggested that these two minerals are part of a homologous series.

Some years earlier, two papers dealt with probable new minerals from the Jílové gold deposit, Czech Republic, and from Megradzorsk, Armenia (Pašava, Breiter, Malátek and Rajlich, 1986; Kovalenker, Zalibekyan, Laputina, Malov, Sandomirskaya, Garasko and Mkhitarayan, 1990). Data did not allow the definition as a new mineral. Obviously the samples are identical with buckhornite. After its acceptance as a new mineral, Johan, Dódony, Morávek and Pašava (1994) published results of a detailed research on buckhornite from the Jílové deposit. Relevant data found by Francis *et al.* (1992) were confirmed in the new paper. In addition, the authors mentioned the partial substitution of Bi by Sb, and a cubic face-centered sub-cell was observed during electron-diffraction studies.

A theoretical model for the atomic arrangement in buckhornite was derived by Effenberger, Paar, Topa, Culetto and Giester (1999). It is based on the crystal structure of nagyagite, $[Pb(Pb,Sb)S_2][(Au,Te)]$, the comparison of cell parameters and chemical composition, and the assumption that nagyagite and buckhornite have structural similarities. Due to lack of proper natural buckhornite, we used synthetic material for a verification of the theoretical model by an experimental crystal-structure analysis. The synthesis of buckhornite was performed during preparative work in the high-temperature superconductive materials search, performed on complex sulfides rather than on the usually investigated oxide ceramics (Culetto, 1997/98).

## Materials synthesis

Buckhornite was synthesized in analogy to nagyagite following the two-step procedure, but at half initial nitrogen pressure, i.e., 0.1 bar $N_2$ atmosphere (see Effenberger *et al.*, 1999). The $AuTe_2$ precursor and analytical or higher grade reagents $Ag_2S$ (FLUKA), Pb (BMG), Bi (FLUKA)

---

* Correspondence author

and S (FLUKA) according to the initial composition $Pb_2BiAg_{0.5}AuS_{3.25}Te_2$ served as input. Later synthesis runs were performed with slightly varied ratios of elements. In total ~1 g sample mass was sealed in a Duran® glass ampulla. It was heated at a rate of 4 K $min^{-1}$ to 660 °C and then at a rate of 2 K $min^{-1}$ to the maximum reaction temperature of 800 °C. Finally, the melt was cooled down to room temperature at a rate of 2 K $min^{-1}$.

Visually, the obtained regulus looked similar to reguli from the nagyagite syntheses (composition of input corresponded to $AgAuSb_3Pb_{13}S_{16}Te_6$). The chemical composition of the reaction products was investigated by an electron-microprobe. Besides buckhornite, the reaction product consists of phases which chemically accord with the minerals treasurite, tetradymite, aleksite, krennerite, petzite, and hessite; additionally some obviously unknown phases were detected. The extremely thin-tabular crystals of chemically homogeneous synthetic buckhornite served for the single-crystal X-ray experiments. The crystals are always bladed on (001). Additional observed faces belong to the crystallographic forms {100}, {010} and rarely to {110}. The crystal plates are extremely lamellar, characteristically they are bent and cleaved. The mechanical instability caused much troubles during search of a single crystal suitable for X-ray investigations.

## Chemical composition

Thin slices of different orientation were cut from the reguli, embedded in resin, ground and polished for the quantitative chemical analyses by electron-microprobe investigations. A JEOL Superprobe 8600, controlled by a LINK-EXL system operated at 25 kV was used (beam current of 30 nA, counting time 20 s). The raw data were processed by the ZAF-4 on-line program. Pure metals ($AuL_\alpha$, $AgL_\alpha$), synthetic $Bi_2Te_3$ ($BiL_\alpha$, $TeL_\alpha$), natural PbS ($PbL_\alpha$, $SK_\alpha$), and $Sb_2S_3$ ($SbL_\alpha$) served as standards. The results are compiled in Table 1.

The chemical composition of buckhornite given by the former authors agrees with our results and the chemical formula is confirmed. Buckhornite is a lead dominated sulfide-telluride, Bi and Au are essential constituents. Like nagyagite, buckhornite has to be considered as a composite structure formed by an alternate stacking of sulfide and telluride layers. In accordance with the investigations by Francis *et al.* (1992) our results show narrow limits for the ratio Pb : Bi = 2 : 1. Johan *et al.* (1994) found natural buckhornite samples with Sb contents up to 3.43 wt%. A minority phase with a composition analogous to buckhornite but with Sb substituting for Bi was observed in samples from nagyagite synthesis runs. The quality of these crystals was insufficient for X-ray investigations. In natural and synthetic samples the ratio Pb : (Bi + Sb) is close to 2 : 1 which indicates an ordered occupation of two distinct crystallographic sites. The ratio Au : Te = 1 : 2 seems to be verified for all natural crystals investigated so far and in all but one of the synthetic samples. The only exception is one sample of our investigation which gave an unexpected ratio of Au : Te = 0.65 : 2.32. In contrast, nagyagite usually has Au : Te ratios essentially smaller than 1 : 2 and samples with Au : Te = 1 : 2 are rare.

## X-ray structure investigation

A huge number of crystal fragments of synthetic buckhornite was checked by Weissenberg and precession film techniques and with a Nonius four-circle diffractometer equipped with a CCD-detector. The major part of crystals showed extremely broad X-ray reflection profiles and multiple splittings even if the optical behaviour suggested sufficient quality. Finally two crystal chips were found to be suitable for structure investigation. The initially determined cell parameters were concurrent within limits of error for both crystals $a = 12.32(1)$ Å, $b = 12.31(1)$ Å and $c = 9.33(1)$ Å, the symmetry is orthorhombic. The only observed extinction rule ($hk0$): $h + k = 2n + 1$ is characteristic for the space groups *Pmmn*, *Pm*2*n* and *P*2*mn*. The structure was solved by direct methods and subsequent difference Fourier summations and it was refined in space group *Pmmn*. During progress of refinements the additional translation vectors ($^1/_3$ 0 0) and ($^2/_3$ 0 0) became evident; they are not demanded by any space group. A great number of reflections ($hkl$) with $h \neq 3n$ were clearly detectable, although their average in-

**Table 1.** Results of electron-microprobe investigations of synthetic buckhornite (sample 1 and 2) and of a chemically related Sb-based compound (sample 3). The average values from # analyses are given (in wt%). In addition the atomic portions were recalculated to a total of 9 atoms corresponding to the number of atoms within the formula unit.

| wt% | # | Pb | Bi | Sb | Ag | Au | S | Te | total |
|---|---|---|---|---|---|---|---|---|---|
| 1 | 35 | 34.6(7) | 19.2(6) | – | – | 16.0(2) | 8.5(6) | 22.5(2) | 100.8 |
| 2 | 8 | 36.3(2) | 18.8(2) | – | – | 11.3(2) | 8.4(1) | 25.9(3) | 100.7 |
| 3 | 12 | 38.6(5) | – | 11.1(2) | 0.26(2) | 9.4(3) | 9.2(1) | 31.1(4) | 99.6 |

| atomic portions | Pb | Bi | Sb | Ag | Au | S | Te | Pb + Bi +Sb + Ag | Au + Te |
|---|---|---|---|---|---|---|---|---|---|
| 1 | 1.93 | 1.06 | – | – | 0.94 | 3.05 | 2.02 | 2.99 | 2.96 |
| 2 | 2.00 | 1.03 | – | – | 0.65 | 3.00 | 2.32 | 3.03 | 2.97 |
| 3 | 1.95 | – | 0.96 | 0.03 | 0.50 | 3.01 | 2.56 | 2.94 | 3.06 |

The Ag contents in the individual analyses of samples 1 and 2 are less than the detection limit of 0.07 wt%. The samples were obtained from synthesis runs with a starting composition of $Pb_2BiAg_{0.5}AuS_{3.25}Te_2$ (sample 1; used for structure investigation), $Pb_2BiAg_{0.33}Au_{0.5}S_3Te_2$ (sample 2) and $Pb_{10.2}Sb_{4.4}AgAuS_{14.8}Te_{8.8}$ (sample 3).

tensity is lower than that of the reflections with $h = 3n$. The attempt to expound these findings by an axial twin was successful: rotating one twin component on [001] by 90° reduced $wR2(F^2)$ and $R1(F)$ from 0.491 and 0.285 to 0.191 and 0.101, respectively. The fractional parts of the two twin components are 0.648(4) and 0.352(4), respectively. A structural investigation of the second crystal chip showed twin components of 0.574(9) and 0.426(9). The structural parameters for both data sets are equal within limits of error. However, the refinement of the second sample yielded somewhat higher R-values. It was concluded that the true cell has $a = 4.108(3)$ Å, $b = 12.308(9)$ Å and $c = 9.331(6)$ Å, the space group *Pmmn* is maintained. For refinements the tripled cell was used and the X-ray scattering contributions of both twin components were considered; the structural parameters of atoms which are equal by translation symmetry were kept constrained.

It is astonishing that Francis *et al.* (1992) had more confidence in the extinction rules determined from powder data than from single-crystal data. Their precession data implied the presence of an *n*-glide plane; the orientation is not quite clear: the extinction symbol is *Pn*-- (from their given extinction rule) or *P*--*n* (from their indexed powder pattern). Additional weak powder lines contradicted the extinction rule. Hence, the authors deduced as possible space groups *Pmmm* and *P*222 (but not *P*2*mm*, *Pm*2*m*, and *Pmm*2). In conformity with the present work the indexed powder pattern given by Johan *et al.* (1994) is consistent with the extinction symbol *P*--*n*. However, the authors mentioned *Pmmm* and *P*222 as the possible space groups for buckhornite. It is unclear, why the polar space groups were excluded from discussion by both groups of authors. The powder patterns of natural buckhornite (Francis *et al.*, 1992, Johan *et al.*, 1994) compare well with that recalculated from the atomic parameters obtained from our structure refinement, despite some details in indexing. The additional weak reflections observed in the pattern given by Francis *et al.* (1992) which violate the extinction rule might be attributed to the contribution of small amounts of impurities. A trial to detect a powder pattern of synthetic buckhornite for a comparison with that taken from the natural material failed. The reguli obtained from syntheses showed an intimate mixture of multiple

**Table 2.** Single-crystal X-ray data collection and structure refinements of synthetic buckhornite, $[Pb_2BiS_3][AuTe_2]$.

| | | | |
|---|---|---|---|
| $a$ | 4.108(3) Å | crystal dimensions | $55 \times 30 \times 4$ μm³ |
| $b$ | 12.308(9) Å | range of data collection | $3° < 2\vartheta < 46.9°$ |
| $c$ | 9.331(6) Å | $\mu$ (Mo$K_\alpha$) | 76 mm$^{-1}$ |
| $V$ | 471.7 Å³ | absorption correction | crystal shape |
| space group | *Pmmn* | total measured reflections | 5421 |
| $Z$ | 2 | observed unique reflections ($n$) | 1135 |
| $\varrho_{calc}$ | 8.25 g cm$^{-3}$ | reflections with $F_o > 4\sigma(F_o)$ | 726 |
| $R_{int} = \sum \lvert F_o{}^2 - F_o{}^2\,(\mathrm{mean})\rvert / \sum F_o{}^2$ | 0.159 | variable parameters ($p$) | 33 |
| $R1 = \sum (\lvert\lvert F_o\rvert - \lvert F_c\rvert\rvert) / \sum F_o$ | 0.101 | GooF $= \{\sum [w(F_o{}^2 - F_c{}^2)^2]/(n-p)\}^{0.5}$ | 1.38 |
| $wR2 = [\sum w(F_o{}^2 - F_c{}^2)^2 / \sum wF_o{}^4]^{0.5}$ | 0.191 | max $\Delta\sigma$ | ≤0.001 |
| extinction parameter | 0.00016(5) | final difference Fourier map | −2.4 to +1.9 e Å$^{-3}$ |

Nonius four-circle diffractometer (CCD-detector, Mo tube, graphite monochromator), unit-cell parameters from least-squares refinements of the $2\vartheta$ values. Data were collected in the $\varphi$-scan mode, scan speed: 0.1°/min; $\Delta\varphi = 2°$/frame; frame size: 621 × 576 pixels, binned mode; detector-to-sample distance: 28 mm. Corrections for Lorentz and polarization effects; neutral atomic complex scattering functions (Wilson, 1992), programs SHELX-76, SHELXS-97, and SHELXL-97 (Sheldrick, 1976, 1997a, 1997b). $w = 1/\{\sigma^2(F_o{}^2) + [0.02^*P]^2 + 90^*P\}$; $P = ([\max(0, F_o{}^2)] + 2^*F_c{}^2)/3]$.

**Table 3.** Structural parameters (e.s.d.'s in parentheses) for synthetic buckhornite. The anisotropic displacement parameters are defined as: $\exp[-2\pi^2 \sum_{i=1}^{3}\sum_{j=1}^{3} U_{ij}\mathbf{a}_i^*\mathbf{a}_j^* h_i h_j]$, $U_{eq}$ according to Fischer & Tillmanns (1988). $U_{12} = U_{13} = 0$ for all atoms.

| Atom | Wyckoff notation | symmetry | $x$ | $y$ | $z$ | $U_{eq}$ |
|---|---|---|---|---|---|---|
| Me(1) | 4(*e*) | *m* | $^1/_4$ | 0.07838(11) | 0.3166(2) | 0.0314(6) |
| Me(2) | 2(*b*) | *mm*2 | $^3/_4$ | $^1/_4$ | 0.6482(2) | 0.0283(7) |
| Au | 2(*a*) | *mm*2 | $^1/_4$ | $^1/_4$ | −0.0045(3) | 0.0201(7) |
| Te | 4(*e*) | *m* | $^3/_4$ | 0.1071(2) | −0.0075(4) | 0.0217(7) |
| S(1) | 2(*b*) | *mm*2 | $^3/_4$ | $^1/_4$ | 0.3654(13) | 0.022(2) |
| S(2) | 4(*e*) | *m* | $^3/_4$ | 0.9123(6) | 0.3835(10) | 0.020(2) |

| Atom | $U_{11}$ | $U_{22}$ | $U_{33}$ | $U_{23}$ | principal mean square displacements of $U$ | | |
|---|---|---|---|---|---|---|---|
| Me(1) | 0.0286(12) | 0.0277(12) | 0.0377(10) | 0.0017(6) | 0.038 | 0.029 | 0.027 |
| Me(2) | 0.0268(14) | 0.0266(13) | 0.0315(12) | 0 | 0.032 | 0.027 | 0.027 |
| Au | 0.0157(11) | 0.0195(12) | 0.0253(11) | 0 | 0.025 | 0.020 | 0.016 |
| Te | 0.0180(15) | 0.0221(13) | 0.0250(14) | 0.0002(14) | 0.025 | 0.022 | 0.018 |
| S(1) | 0.022(7) | 0.017(7) | 0.027(6) | 0 | 0.028 | 0.022 | 0.017 |
| S(2) | 0.014(5) | 0.019(5) | 0.025(4) | 0.002(3) | 0.026 | 0.019 | 0.014 |

**Table 4.** Interatomic bond distances (in Å) and bond angles (in °) for synthetic buckhornite.

| | | | | | |
|---|---|---|---|---|---|
| Me(1)–S(2)$^a$ | 2.800(11) | | S(2)$^a$–Me(1)–S(2)$^b$ | 79.5(2) | 2× |
| Me(1)–S(2)$^b$ | 2.964(7) | 2× | S(2)$^a$–Me(1)–S(1) | 79.5(3) | 2× |
| Me(1)–S(1) | 2.981(4) | 2× | S(2)$^b$–Me(1)–S(2)$^b$ | 87.8(3) | |
| Me(1)–Au | 3.665(7) | | S(2)$^b$–Me(1)–S(1) | 88.7(2) | 2× |
| Me(1)–Te | 3.673(7) | 2× | S(2)$^b$–Me(1)–S(1) | 159.0(3) | 2× |
| Me(1)–Te | 3.677(7) | | S(1)–Me(1)–S(1) | 87.2(2) | |
| Me(2)–S(1) | 2.638(14) | | S(1)–Me(2)–S(2) | 84.1(2) | 4× |
| Me(2)–S(2) | 2.880(6) | 4× | S(2)–Me(2)–S(2) | 87.8(3) | 2× |
| Me(2)–Te | 3.663(7) | 2× | S(2)–Me(2)–S(2) | 91.0(3) | 2× |
| Me(2)–Au | 3.838(7) | 2× | S(2)–Me(2)–S(2) | 168.2(4) | 2× |
| Au–Te | 2.705(4) | 4× | Te–Au–Te | 81.1(2) | 2× |
| Au–Me(1) | 3.665(7) | 2× | Te–Au–Te | 98.9(2) | 2× |
| Au–Me(2) | 3.838(7) | 2× | Te–Au–Te | 178.8(3) | 2× |
| Te–Au | 2.705(4) | 2× | Au–Te–Au | 98.9(2) | |
| Te–Te$^a$ | 3.343(7) | 2× | Au–Te–Te$^a$ | 92.6(2) | 2× |
| Te–Te$^b$ | 3.517(10) | | Au–Te–Te$^a$ | 168.1(1) | 2× |
| Te–Me(2) | 3.663(7) | | Te$^a$–Te–Te$^a$ | 75.9(2) | |
| Te–Me(1) | 3.673(7) | 2× | | | |
| Te–Me(1) | 3.677(7) | | | | |
| Te–S(1) | 3.898(13) | | | | |
| Te–S(2) | 4.073(11) | 2× | | | |
| S(1)–Me(2) | 2.638(14) | | Me(2)–S(1)–Me(1) | 98.8(2) | 4× |
| S(1)–Me(1) | 2.981(4) | 4× | Me(1)–S(1)–Me(1) | 87.2(2) | 2× |
| | | | Me(1)–S(1)–Me(1) | 90.2(2) | 2× |
| | | | Me(1)–S(1)–Me(1) | 162.4(3) | 2× |
| S(2)–Me(1)$^a$ | 2.800(10) | | Me(1)$^a$–S(2)–Me(2) | 97.5(2) | 2× |
| S(2)–Me(2) | 2.880(6) | 2× | Me(1)$^a$–S(2)–Me(1)$^b$ | 100.5(2) | 2× |
| S(2)–Me(1)$^b$ | 2.964(7) | 2× | Me(2)–S(2)–Me(2) | 91.0(3) | |
| | | | Me(2)–S(2)–Me(1)$^b$ | 87.8(2) | 2× |
| | | | Me(2)–S(2)–Me(1)$^b$ | 162.0(3) | 2× |
| | | | Me(1)$^b$–S(2)–Me(1)$^b$ | 87.8(3) | |

phases. An unambiguous indexing was therefore impossible. The intensely intergrown compounds did not allow the reasonable separation of single phases in a sufficient amount. Consequently the refinements of the cell parameters from powder data failed.

Cell metrics as well as details on data collection and structure refinements are summarized in Table 2. Structural data given in Table 3 refer to the true cell of (synthetic) buckhornite. Interatomic bond lengths and bond angles are summarized in Table 4. Due to the similar X-ray scattering power it is impossible to discriminate experimentally the occupation of the two Me positions by Pb or Bi atoms. The distinct crystal chemical features of the two elements and the analytically detected ratio Pb : Bi = 2 : 1 support the suggestion that the Me(1) and Me(2) positions are (dominantly) occupied by Pb and Bi atoms, respectively.

## Results and discussion

As proposed by Francis *et al.* (1992), Johan *et al.* (1994) and Effenberger *et al.* (1999) buckhornite and nagyagite can indeed be considered as parts of a homologous series. This becomes evident if the cell content of buckhornite, $2 \times \{[(\mathrm{Pb_2Bi})_{\Sigma3}\mathrm{S_3}][(\mathrm{AuTe_2})_{\Sigma3}]\}$, is compared with that of the tripled average nagyagite cell, $2\times \{[(\mathrm{Pb_3(Pb,Sb)_3})_{\Sigma6}\mathrm{S_6}][(\mathrm{Au},\underline{\mathrm{Te}})_3]\}$. The buckhornite cell and the average nagyagite cell can be compared to each other: $a_{\mathrm{buckhornite}} \sim a_{\mathrm{nagyagite}}$, $b_{\mathrm{buckhornite}} \sim 3 \times b_{\mathrm{nagyagite}}$, $c_{\mathrm{buckhornite}} = c_{\mathrm{nagyagite}} - 5.797$ Å; the difference in $c$ corresponds roughly to twice the Pb/Bi/Sb–S bond distance. Both compounds feature pronounced layer structures composed of two structural units parallel to (001). In buckhornite *two* (Pb,Bi)S sheets form a one slab thick SnS-archetype (Makovicky, 1993). It is intercalated between gold-tellurium layers; they consist of planar $^1_\infty\mathrm{AuTe_2}$ ribbons. In nagyagite *four* (Pb,Sb)S layers form a slice with a thickness of two SnS-archetype slabs which is sandwiched between the gold-tellurium layers (Fig. 1; all atomic arrangements were drawn with the program ATOMS, Dowty, 1997). The structural data on nagyagite mentioned in the present paper refer to Effenberger *et al.* (1999).

The crystal structure of buckhornite is shown in Fig. 2. Within the $^2_\infty[\mathrm{Pb_2BiS_3}]$ layer two crystallographically different cation positions Me(1) and Me(2) occur. Both have five S atoms within the first coordination sphere. The coordination figures are tetragonal pyramids. The Me–S bond distances to the apices are shorter than those to the four S atoms of the basal plane. The cations are shifted out of the square towards the gold-tellurium layer. Thus, a one-sided coordination figure is formed which allows to adopt for the space requirements of the lone-pair electrons of the cations Pb(II) and Bi(III). However, both size and shape of the two MeS$_5$ polyhedra are slightly distinct from each other. The Me(1)S$_5$ polyhedron is larger than the Me(2)S$_5$ polyhedron with respect to the bonds to the

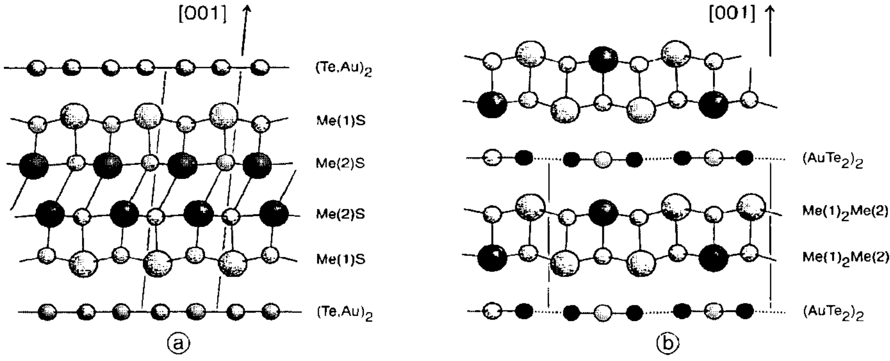

**Fig. 1.** The two members forming a homologous series with $^{2}_{\infty}[(Pb,Bi,Sb)S]_n$ and (Au,Te) layers. (**a**) Nagyagite ($n = 2$): Me(1) = Pb, Me(2) = (Pb,Sb); Au und Te are indistinguishable in the average cell. (**b**) Buckhornite ($n = 1$): Me(1) = Pb, Me(2) = (Bi,Sb); the $^{1}_{\infty}AuTe_2$ ribbons are indicated. The composition for the separate layers is given with respect to the unit cells.

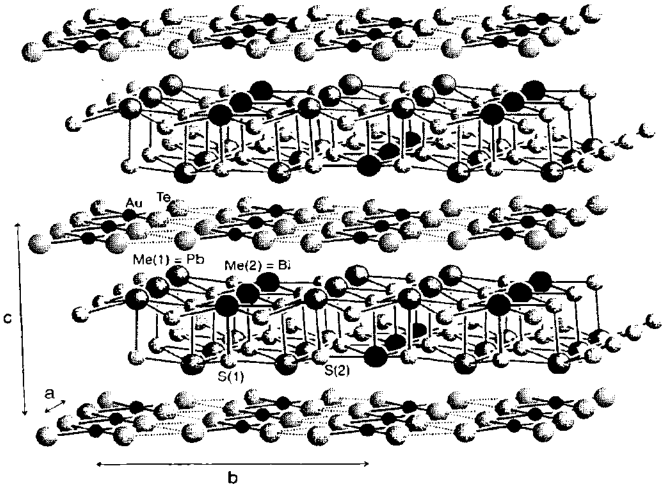

**Fig. 2.** The crystal-structure of buckhornite formed by SnS-archetype layers $^{2}_{\infty}[Pb_2BiS_3]$ separated by $^{1}_{\infty}AuTe_2$ ribbons.

apices (2.80 Å and 2.64 Å) and to those within the basal square (2.97 Å and 2.88 Å). The gap within the [1 + 4] coordination is smaller for the Me(1)$S_5$ polyhedron (0.17 Å) than for the Me(2)$S_5$ polyhedron (0.24 Å). The elevation of the Me atom from the basal $S_4$ plane is larger for Me(1) [0.541(9) Å] than for Me(2) [0.295(9) Å]. The site symmetries of the positions Me(1) and Me(2) are *m* and *mm*2, respectively. A distinction between the atoms Pb and Bi is impossible by conventional X-ray scattering experiments. However, from crystal chemical expectations it is most likely that the position Me(1) is predominantly occupied by Pb atoms; vice versa the position Me(2) should be predominantly occupied by Bi (and Sb) atoms. The Me(1)$S_5$ polyhedron compares with the Me(1)$S_5$ = $PbS_5$ polyhedron in nagyagite. Separation of Pb and Bi into two atomic positions correlates with the chemical data because the ratio Pb:(Bi + Sb) is close to the ratio of the site multiplicities Me(1):Me(2) = 2:1. In sulfides containing Pb and Bi an at least partial separation of the two atoms at positions with different size of the coordination polyhedra was often found: (c.f. Kupčik, 1984, Makovicky *et al.*, 1991, 1992 or Bente, Engel and Steins, 1993 and references therein). According to Makovicky (1981) an exact [1 + 4] coordination for Bi atoms is unusual. In buckhornite the displacement parameters of all atomic sites and especially of the Me(2) atom and of the adjacent S atoms are as usual; they do not indicate a static or dynamic disorder to achieve an asymmetry of the coordination polyhedra. The regular coordination might be stabilized by the weak interaction between the Me(1) and Me(2) atoms with their additional Te ligands.

The sulfide layer in buckhornite features a package of one SnS-archetype slab. In nagyagite the sulfide layer is twice as thick and it is formed by two SnS-archetype slabs (see Fig. 1). The layer sequences are $Me(1)_2Me(2)S_3$–$Me(1)_2Me(2)S_3$ and Me(1)S–Me(2)S–Me(2)S–Me(1)S in the two compounds. Analogous SnS archetype layers were found in several chalcogenides, among them are some composite incommensurate structures (socalled "misfits"). Within the cylindrite-franckeite homologous series similarly one and two slabs of the SnS-archetype are sandwiched between pseudohexagonal layers (Makovicky and Hyde, 1992, Lafond, Meerschaut, Moëlo, and Rouxel, 1996, Lafond, Nader, Moëlo, Meerschaut, Briggs, Perrin, Monceau and Rouxel, 1997). Further examples are $TiPbSbS_3$ (Balić Žunić, Bente and Edenharter, 1992, Balić Žunić and Bente, 1995) or the mineral lengenbachite (Makovicky, Leonardsen and Moëlo, 1994). Recently investigations on the synthetic compounds $\sim[(Pb,Sb)_2S_2][NbS_2]$ and $[(Pb_{1.82}Sb_{0.46})_{\Sigma=2.28}S_{2.28}][NbS_2]$ were performed by Lafond *et al.* (1996, 1997). Surveys are given by Makovicky and Hyde (1992) and by Wiegers and Meerschaut (1992).

Although only the average structure of nagyagite was determined by Effenberger *et al.* (1999), there is no doubt on the principal uniformity of the gold-telluride layer in buckhornite and nagyagite. In the average nagyagite structure Te and Au paradoxically have to be assigned to one atomic position with site symmetry *m*. From this occupation resulted a formal square-planar (Te,Au) net. In nagyagite Au:Te varies on a wide scale (it scatters in most analyses roughly from 1:2 to 1:3), in buckhornite the ratio Au:Te is close to 1:2. In buckhornite an ordering of the Au and Te atoms on two different crystallographic sites with site symmetries *mm*2 and *m* was observed. The symmetry elements *m* and 2 are perpendicular to the gold-tellurium layers. The experimental results fully correspond with the theoretical model proposed by Effenberger *et al.* (1999). The Au atoms are [4] coordinated with Au–Te bond distances of 2.71 Å. The coordination figure is practically planar. This coordination is in agreement with the valence state (III) as proposed by Johan *et al.* (1994). It further agrees with the environment in Au(III) telluride halides with Au–Te ≈ 2.68 Å (Haendler, Mootz, Rabenau

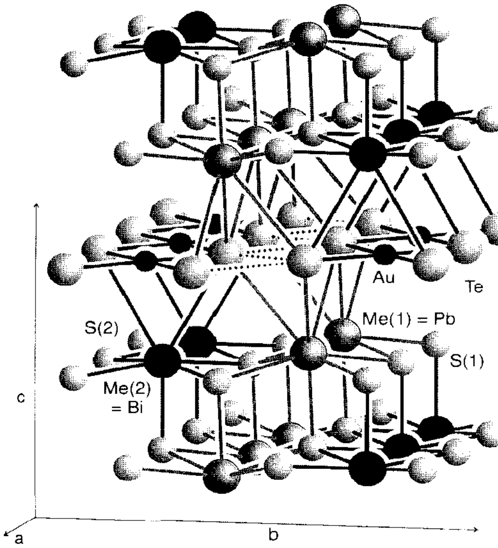

**Fig. 3.** The connection between the SnS-archetype layers ${}^{2}_{\infty}[Pb_2BiS_3]$ and the ${}^{1}_{\infty}AuTe_2$ ribbons in the crystal-structure of buckhornite: the weak Me(1)—Te and Me(2)—Te bonds are shown.

and Rosenstein, 1974, Fenner and Mootz, 1978). The $AuTe_4$ configuration in buckhornite share each two *trans*-arranged Te—Te edges to form ribbons with the formula ${}^{1}_{\infty}AuTe_2$. This connection causes a distortion of the $AuTe_4$ squares: the Te—Au—Te bond angles are 81 and 99°, respectively. The Te—Te distances are 3.52 Å and 4.11 Å for the shared and unshared edges within the $AuTe_4$ configuration. The Te—Te distances between the $AuTe_2$ ribbons are 3.34 Å and indicate weak Te—Te contacts. It is remarkable that they are shorter than the Te—Te edges within the $AuTe_4$ configuration. Further they are shorter than the additional bonds in native tellurium. Native tellurium (Adenis, Langer and Lindqvist, 1989) consists of infinite helices with Te—Te = 2.835 Å (2×) and Te—Te—Te = 103.14°, additional bonds are 3.491 Å (4×). In nagyagite the average (Te,Au)—(Te,Au) distance of 2.97 Å features statistically a mean value of Au—Te and Te—Te lengths.

The cell direction $b$ shows a pronounced pseudotranslation. Neglecting the differences in stereochemistry of the coordination polyhedra around the atom pairs Pb/Bi and Au/Te, a pseudocell with $b_{\text{pseudocell}} = {}^{1}/_{3} \times b_{\text{true cell}}$ is obtained. In addition, the scattering power of the Pb and Bi atoms is indistinguishable by conventional X-ray sources, at least at the present accuracy of X-ray structure refinements. As a consequence, the X-ray reflections $hkl$ with $k \neq 3n$ are weak (average value of $F_o$ is 98.4) as compared to the reflections $hkl$ with $k = 3n$ (average value of $F_o$ is 348.2).

Weak interactions between the ${}^{2}_{\infty}[Pb_2BiS_3]$ layers with a charge donor character and the anionic ${}^{1}_{\infty}AuTe_2$ ribbons are evident (Fig. 3). Formally this causes a completion of the coordination of the Me(1) and Me(2) atoms. But the cation—cation and anion—anion interlayer distances are of similar length as cation—anion distances of the second coordination sphere. The long distances of about 3.7 Å reflect primarily Van der Waals contacts with the electron pair in the interspace. The weak interactions are responsible for the extremely laminated to foliated habit and the mechanical instability of buckhornite which caused much troubles during search for a crystal chip suitable for structure investigation.

*Acknowledgments.* We want to express our gratitude to Prof. E. Tillmanns, Prof. E. Makovicky and Prof. K. Bente for fruitful comments and suggestions which improved the paper. F. J. C. thanks Mr. H. Goger and Mr. J. Sitter for technical assistance.

## Reference

Adenis, C.; Langer, V.; Lindqvist, O.: Reinvestigation of the structure of tellurium. Acta Crystallogr. **C45** (1989) 941 942.

Balić Žunić, T.; Bente, K.: The two polymorphs of $TlPbSbS_3$ and the structural relations of phases in the system $TlSbS_2$—PbS. Mineral. Petrol. **53** (1995) 265–276.

Balić Žunić, T.; Bente, K.; Edenharter, A.: Crystal structures of high temperature thallium lead antimony sulfide, $Tl_{0.333}Pb_{0.333}Sb_{0.333}S$. Z. Kristallogr. **202** (1992) 145–146.

Bente, K.; Engel, M.; Steins, M.: Crystal structure of lead silver tribismuth sulfide, $PbAgBi_3S_6$. Z. Kristallogr. **205** (1993) 327–328.

Culetto, F. J.: Materials Synthesis for the KELAG-HTc-Project, KELAG — Kärntner Elektrizitäts — Aktiengesellschaft, Klagenfurt. Internal Summary Report, 1997/98.

Dowty, E.: ATOMS 3.2. A Computer Program for Displaying Atomic Structures, Kingsport, TN 37663, 1997.

Effenberger, H.; Paar, W. H.; Topa, D.; Culetto, F. J.: Giester, G.: Toward the crystal structure of nagyagite, $[Pb(Pb,Sb)S_2][(Au,Te)]$. Amer. Mineral. **84** (1999) 669–676.

Fenner, J.; Mootz, D.: The crystal structure of gold telluride iodide AuTeI. J. Solid State Chem. **24** (1978) 367–369.

Fischer, R. X.; Tillmanns, E.: The equivalent isotropic displacement factor. Acta Crystallogr. C**44** (1988) 775–776.

Francis, C. A.; Criddle, A. J.; Stanley, C. J.; Lange, D. E.; S'how Shieh; Francis, J. G.: Buckhornite, $AuPb_2BiTe_2S_3$, a new mineral species from Boulder County, Colorado, and new data for aikinite, tetradymite and calaverite. Canad. Mineral. **30** (1992) 1039–1047.

Haendler, H. M.; Mootz, D.; Rabenau, A.; Rosenstein, G.: The crystal structures of $AuTe_2Cl$ and $AuTe_2I$. J. Solid State Chem. **10** (1974) 175–181.

Johan, Z.; Dódony, I.; Morávek, P.; Pašava, J.: La buckhornite, $Pb_2Au \cdot BiTe_2S_3$, du gisement d'or de Jílové, République tchèque. Compt. Rend. Acad. Sci. Paris, Sér. II **318(9)** (1994) 1225–1231.

Kupčik, V.: Die Kristallstruktur des Minerals Eclarit, $(Cu,Fe)Pb_9Bi_{12}S_{28}$. Tschermaks Mineral. Petrogr. Mitt. **32** (1984) 259–269.

Kovalenker, V. A.; Zalibekyan, M. A.; Laputina, I. P.; Malov, V. S.; Sandomirskaya, S. M.; Garasko, M. I.; Mkhitarayan, D. V: Minéralisation sulfuro-tellurée du district de Megradzorsk en Arménie. Geol. Rudnych Mestorozd **3** (1990) 65–81.

Lafond, A.; Meerschaut, A.; Moëlo, Y.; Rouxel, J.: Premier composite bicouche incommensurable de type franckéite dans le système Pb—Sb—Nb—S. Comp. Rend. Acad. Sci. Paris, Sér. II b **322** (1996) 165–173.

Lafond, A.; Nader, A.; Moëlo, Y.; Meerschaut, A.; Briggs, A.; Perrin, S.; Monceau, P.; Rouxel, J.: X-ray structure determination and superconductivity of a new layered misfit compound with a frankeite-like stacking $[(Pb,Sb)S]_{2.28}NbS_2$. J. All. Comp. **261** (1997) 114–122.

Makovicky, E.: The building principles and classification of bismuth-lead sulphosalts and related compounds. Fortschr. Mineral. **59** (1981) 137–190.

Makovicky, E.: Modular classification of sulfosalts — current status. Definition and application of homologous series. N. Jahrb. Mineral. Abhandl. **160** (1989) 269–297.

Makovicky, E.: Rod-based sulphosalt structures derived from the SnS and PbS archetypes. Europ. J. Mineral. **5** (1993) 545–591.

Makovicky, E.; Hyde, B. G.: Incommensurate, two-layer structures with complex crystal chemistry: minerals and related synthetics. Mater. Sci. Forums **100&101** (1992) 1–100.

Makovicky, E.; Leonardsen, E.; Moëlo, Y.: The crystallography of lengenbachite, a mineral with the non-commensurate layer structure. Neues J. Mineral. Abh. **166** (1994) 169–191.

Makovicky, E.; Mumme, W. G.; Hoskins, B. F.: The crystal structure of Ag–Bi-bearing heyrovskyite. Canad. Mineral. **29** (1991) 553–559.

Makovicky, E.; Mumme, W. G.; Madsen, I. C.: The crystal structure of vikingite. Neues J. Mineral. Monatsh. **1992** (1992) 454–468.

Pašava, J.; Breiter, K.; Malátek, J.; Rajlich, P.: Cu-rich rucklidgeite and an unnamed Pb–Au–Bi sulphosalttelluride from the gold deposit Jílové u Prahy. Věst. Ústř. Útavu Geol. **61** (1986) 217–221.

Sheldrick, G. M.: SHELX-76 Programs for Crystal Structure Determination, University Cambridge, England 1976.

Sheldrick, G. M.: SHELXS-97, a program for the solution of crystal structures. University Göttingen, Germany 1997a.

Sheldrick, G. M.: SHELXL-97, a program for crystal structure refinement. University Göttingen, Germany 1997b.

Wiegers, G. A.; Meerschaut, A.: Misfit layer compounds $(MS)_nTS_2$ ($M = Sn$, Pb, Bi, rare earth metals; $T = Nb$, Ta, Ti, V, Cr; $1.08 < n < 1.23$): structures and physical properties. Mater. Sci. Forums **100&101** (1992) 101–172.

Wilson, A. J. C. (ed.): *International tables for crystallography.* Vol. C, mathematical, physical and chemical tables, 883 pages, Kluwer Academic Publishers, Dordrecht, Boston, London 1992.